Simultaneous FDM 4D Printing and Magnetizing of Iron-Filled Polylactic Acid Polymers

Mahmoud Moradi[1], Mohammadreza Lalegani Dezaki[2], Erfan Kheyri[3], Seyyed Alireza Rasouli[3], Milad Aghaee Attar [4] and Mahdi Bodaghi[2,*]

[1] *Faculty of Arts, Science and Technology, University of Northampton, Northampton NN1 5PH, UK*

[2] *Department of Engineering, School of Science and Technology, Nottingham Trent University, Nottingham NG11 8NS, UK*

[3] *Department of Mechanical Engineering, Faculty of Engineering, Malayer University, Malayer, Iran*

[4] *Department of Mechanical Engineering, Faculty of Engineering, K.N. Toosi University of Technology, Tehran, Iran*

*Corresponding author: mahdi.bodaghi@ntu.ac.uk

Abstract

4D printing magnetic structures with excellent strength activated with a low level of the magnetic field is always desired but challenging. This work studies the influence of simultaneous magnetization on the magneto-mechanical performance of 4D-printed active polymers. The main aim is to magnetise magnetic iron polylactic acid (PLA) material during 4D printing via fused deposition modelling (FDM) process. During the printing process, the magnetization of the samples is performed in various magnetic field states. Specimens are printed in three states with two magnets around the printing area, magnets under the printing area, and without magnets, at three angles of 0, 45, and 90° to the applied magnetic field. Vibrating sample magnetometer (VSM), mechanical tests, and scanning electron microscope (SEM) are used to investigate the effects of the applied magnetic field on the magnetization with different printing conditions, mechanical properties of different printing angles, and the microstructure of printed samples. Results show that printed samples on the edge of the magnet are saturated in a higher specific magnetization compared to the printed samples with magnets around and without a magnetic field. The specific magnetization in the magnetic field in the direction of the sample deposition increases by 63.46% by applying a magnetic field. The strength increases 21.4% when a magnetic field is present, and the sample is printed at 0° angle along the tension direction. The printed sample has better mechanical properties when two magnets are used around the printing region rather than one under it, which is independent of the impact of the printing angle. Finally, the optimal printing mode for obtaining the appropriate magnetic and mechanical characteristics is 3D printing with magnets under the printing bed at 0° angle along the tension direction.

Keywords: Additive Manufacturing; 4D Printing; Fused Deposition Modelling; Magneto-active polymers; Iron-filled PLA

1. Introduction

Currently, additive manufacturing (AM) process competes with many conventional manufacturing methods in terms of cost, speed, reliability, and accuracy. The advantages of AM include high production speed, freedom of design, saving money, and green production [1]. FDM is the most common material extrusion technology of the 3D printing type [2,3]. The variety of materials and the excellent mechanical qualities of the items produced using this technique are FDM's key strengths [4].

A filament-based material 3D printing extrusion process known as FDM is one in which a polymer filament is melted using a heated nozzle and carefully dispensed layer by layer to create parts [5,6]. Thermoplastic polymers used for FDM must be converted into a series of filaments and then prepared for 3D printing. In FDM, a variety of polymer-based materials and smart materials can be utilised, however polylactic acid (PLA) usage is highly common [7]. 4D printing creates 3D objects using the same techniques as 3D printing which is material deposition directed by computer programming. 4D printing of smart materials can produce flexible parts with dynamic structures. These parts have interesting features such as folding, unfolding, self-twisting, self-inflation, and self-assembly [8–10]. In general, the 4D printing of smart materials can be used in medical applications, soft robotics, self-evolving structures, active origami, sensors, and flexible electronics [11,12]. The printed object responds to factors like tension, pressure, temperature, pH, and electric or magnetic field [13,14].

Responsive magnetomaterials are smart objects that react to magnetic fields. For instance, magnetic fields and magnetic nanoparticles can be used to establish remote control in a micro-receiver made from hydrogels or silicones [15–17]. In these materials, embedding occurs during pre-processing. Metal and polymer printing applications for this technique are quite promising. Hence, the printed sample reacts to the external magnetic field. Magnetic polymer materials can be printed using FDM technology due to its features in terms of printing composite materials [18]. Among the many potential types of devices and actuation modes, magnetically responsive materials are particularly exciting since they are rapid, contactless, and driven by magnetic fields that may be used safely near humans [19,20]. The specific applications of 4D-printed magneto-responsive materials are shape morphing [21], bone scaffold structure [22], metamaterial structures [23], shape locking systems [24], and grippers [25].

Henderson et al. [26] investigated the modification of the magnetic properties of PLA iron filament using magnetic field-assisted AM. In this research, three different samples of Protopasta magnetic materials, a combination of iron and polylactic acid (PLA), were printed in the presence of a magnetic field and then measured using a vibrating sample magnetometer (VSM) to determine the printing effects in on the magnetic properties of the samples. The magnetic programming of printed shape memory composite structures was researched by Zhang et al. [22]. In this work, several structures were printed using PLA and composite filaments comprised of Fe_3O_4 and PLA which are biocompatible and biodegradable. Investigations were made into the shape memory characteristics of printed objects produced by magnetic fields. Analyses of mechanical and thermodynamic characteristics were conducted. Under a certain temperature and magnetic field, the form recovery mechanism was identified.

A bioprocess-inspired tracheal frame idea using magnetically stimulated shape memory composites was described by Zhao et al. [27]. This article explained how shape memory polymer (SMP) is used in the custom 4D printing of tracheal framework that is made using biological models. This article suggested a brand-new manufacturing technique and idea for individually modifying tube frames with irregular shapes. Two bio-inspired frameworks are fabricated through the printing of PLA/Fe_3O_4 composite. The created scaffolds could be inserted into the body in a momentarily deformed configuration and then be exposed to an alternating magnetic field to restore them to their original shape. Multi-material magnetic printing for multimodal shape conversion with tunable properties and switchable mechanical behaviours was studied by Ma et al. [28]. To study the multimodal deformation and better tunable features of soft magnetic materials and magnetic shape memory polymers, researchers created a multi-material printing process. They demonstrated multiple deformation modes with distinct shape configurations using combined thermal and magnetic excitation, enabling more active metamaterials with controllable physical properties. Also, active magnetic soft materials for on-demand magnetic stimulation conversion were created by Zhang et al. [19]. Printed magnetically active soft material with 3D patterned magnetic profile, programmable deformation, and controllable motion showed promising applications in actuators and soft robotics. They also demonstrated the diverse functions resulting from the complex deformation of robots.

According to previous studies in this field, the impact of the printing angle compared to the angle of the magnetic field lines applied during the printing procedure, on the magnetic and mechanical properties of the printed samples, has not been explored. In this research, the effects of the magnetic field during the 4D printing procedure of smart magnetic filament are discussed. The initial goal of this study is to look at how the presence of a magnetic field affects the mechanical and magnetic properties of 4D-printed samples. The proposed study is useful in stimulating 4D-printed structures with optimum parameters. Shape changing with less magnetic power and stronger 4D scaffolds can be obtained using this technique.

For this purpose, the FDM 3D printing method is used to extrude iron PLA magnetic smart filament. The printer in this study has been modified to apply the magnetic field while printing samples. Different angles and magnetic field conditions are used to test the magnetic characteristics of printed samples. Several magnet positioning states are employed to create magnetic fields. The effects of varied printing angles at 0, 45, and 90° with respect to the magnetic field's direction and the desired tension direction are investigated as well. A tensile test is then performed on the manufactured samples to examine the impact of the magnetic field on the mechanical characteristics of printed samples at various printing angles. The fracture parts of the chosen samples are then photographed for a more thorough study.

2. Materials and methods

This section introduces the research's equipment and provides an explanation of the procedures and tests run. The necessary steps to prepare the devices and samples are explained after the introduction of the tools and devices used.

2.1. Materials

In general, two types of filaments were used in this research. The filament studied in this research is the smart magnetic PLA filament filled with iron (around 15 wt%). Also, acrylonitrile butadiene styrene (ABS) filament was used to make the magnets holder. Iron PLA filament manufactured by Protopasta Company was used. This oxidizable filament is a ferromagnet material that responds to a magnet field and has the same behaviour as pure iron. Encased in plastic, the iron particles retain a stable cast and matte finish when printed but can be oxidized if desired to print rusted decorative parts. This filament is more abrasive than standard PLA. It is preferable to switch to a wear-resistant nozzle or a nozzle with a bigger diameter while printing with this filament to extend service intervals. ABS PLUS filament manufactured by Net3d company was used to make the magnet holder and other parts. This filament has lower dimensional accuracy and higher melting temperature than PLA and is more economical.

2.2. Magnet holder

Two magnet holders were designed using SolidWorks software to match the size of the magnets to maintain two magnets around the printer nozzle to provide a magnetic field while printing samples. The holders were manufactured by the printer itself. For installation on the printer's x-axis, these two holders were created as shown in Figure 1(a).

2.3. FDM modifications and printing parameters

FDM printer is used to print all samples due to its capability is printing thermoplastic with good surface quality and mechanical properties [29,30]. Also, printing composite materials can be achieved using this technique [31–33]. The open-source FDM printer was used to print the samples as shown in Figure 1(b). This printer used a direct extruder to extrude melted materials and can print parts in dimensions of length, width, and height of up to 50 cm. The printer was customized to print samples in different magnetic field conditions. The FDM printer used in the study was modified to print samples under various magnetic field conditions. Additionally, to achieve an acceptable print quality, the printing parameters had to be adjusted based on the characteristics of the magnetic field that was being applied to the samples being printed.

Since the protective part of the extruder cooling fan was unable to keep the holders stationary and moving due to the magnets present as well as the pressure created by the weight of the magnets and holders, the holders were permanently mounted on the printer's x-axis aluminium profile. The end-stop collision sensor module of the printer was then moved to the top of the holder, on the profile, in accordance with the reduction of the extruder's range of motion in the x-axis, between the two holders, to prevent the extruder from striking the holders.

Additionally, five mirror layers were employed underneath the print sample to ensure that the printing process occurs in the magnet's core. To keep the mirrors from shifting during the printing of the prototypes, they were joined at the sides using regular hot glue. In general, the same requirements had to be satisfied to print the samples in the three different circumstances of printing without a magnet, printing with a magnet around the printing area, and printing with a magnet underneath the sample.

At first, using a nozzle of 0.6 mm, due to better quality, we decided to use the parameters of extrusion temperature of 245 °C, bed temperature of 45 °C, layer thickness of 0.25 mm, and printing speed of 35 mm/s. However, due to the lack of the mixing of the appropriate layer and due to the interruption of the printing process, and the creation of errors during the printing process in the state of the magnet below, it was not possible to use the said parameters. Finally, by using the trial-and-error method, the optimal parameters for printing tensile test samples in three magnetic conditions were obtained. The 230 °C nozzle temperature, 45 °C bed temperature, 0.5 mm layer thickness, and 35 mm/s printing speed were found to be applicable in all three scenarios without prior issues.

The printing of tensile test samples on magnets has undergone yet another optimization. The magnets were relocated to the bottom of the tray because the melt being extruded not being stable, the correct layer not being mixed, the extruder fan's cooling function failed, and the inability to print directly on the magnet (see Figures 2(a) and (b)).

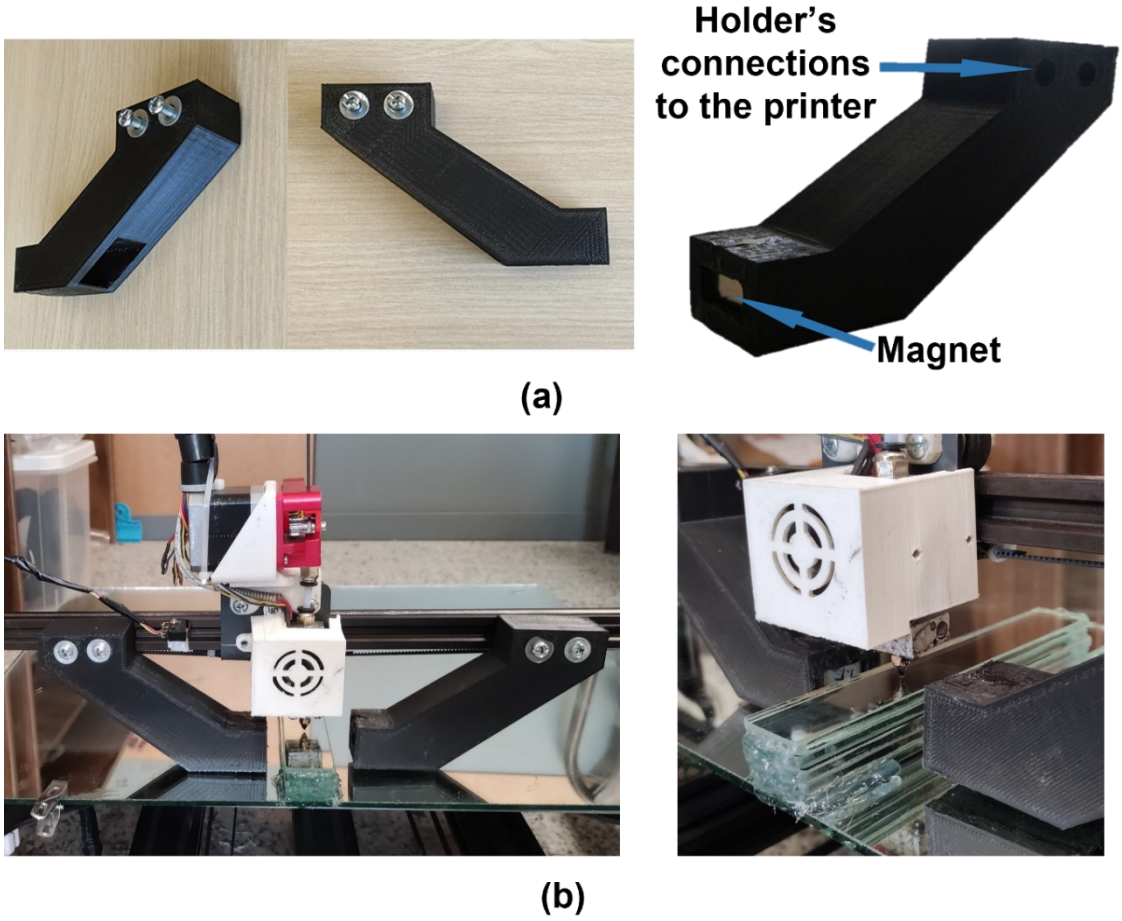

Figure 1. (a) Built-in magnet holder for mounting on the printer. **(b)** The personalized part of the printer for printing samples with magnets around.

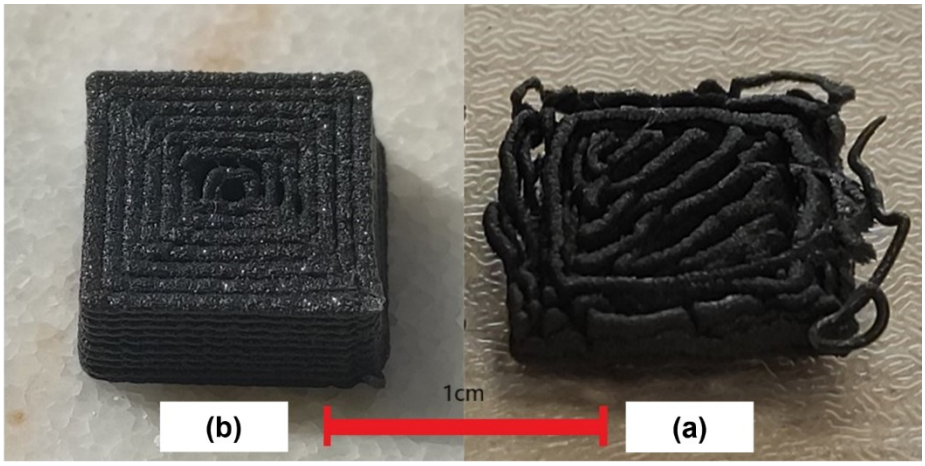

Figure 2. Pre-printed tests: a) cube sample printed on the magnet with initial temperature and b) cube sample printed on the mirror with magnets under the tray and optimized temperature.

2.4. Vibrating sample magnetometer (VSM)

One of the ways to induce a magnetic field is to use permanent magnets. In this research, permanent block neodymium magnets of grade N52 with dimensions of 20 x 20 x 10 mm from First4Magnet were used. Different samples were printed in various magnetic field conditions for VSM measurements to examine how the magnetization of the samples changed while they were in the various states of magnetic fields. Additionally, multiple samples were printed with varied angles of the printing lines relative to the stretching direction of the tensile test to evaluate the impact of magnetic field conditions on the mechanical characteristics of the printed sample.

Samples were printed in three states with a magnet surrounding the printing region, a magnet below, and without a magnet at three angles to the lines of the applied magnetic field to examine the change in magnetization of the samples during printing. According to previous studies [34], the printing parameters were 0.6 mm nozzle diameter, 200 °C nozzle temperature, 45 °C bed temperature, 30 mm/s printing speed, and 0.5 mm outer shell layer thicknesses. Due to the dimensional limitation of the VSM device, the samples were printed in three layers with a length of 5 mm (see Figure 3(a)).

Five samples were printed first at the parameters to verify the impact of the magnetic field on the magnetization of the printed samples under the influence of the field. In the next step, by checking the results and ensuring the effectiveness of the magnetic field on the magnetic properties of the printed samples, the previous conditions were completed and for further investigation, the samples were also printed with the conditions as shown in Table 1. Note that a hypothetical line was put on the magnet to separate states E and F from one another (see Figure 3(b)).

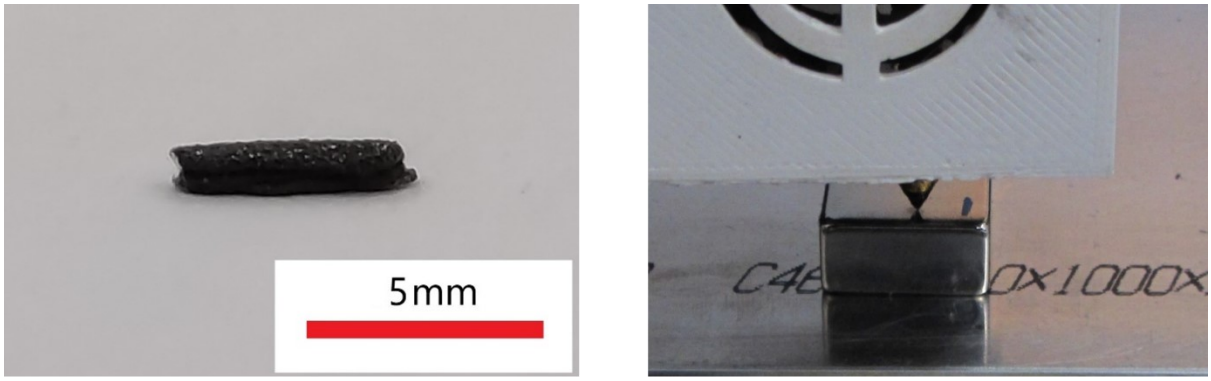

Figure 3. (a) Printed VSM sample. **(b)** Printing in E and F modes.

Table 1. Schematic figures of printed VSM samples (grey lines represent field lines)

State	Printing mode	Schematic image of printed samples
A	Printing without any magnetic field	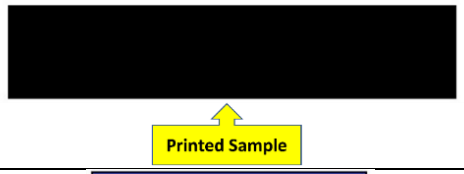
B	Printing with a magnet around the printed area perpendicular to the field lines	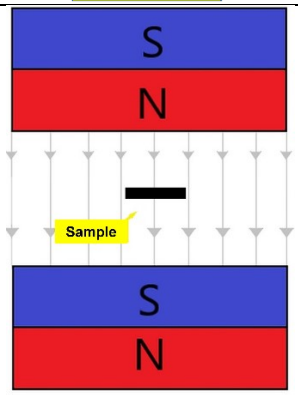
H	Printing with a magnet around the printed area at 0° to the field lines	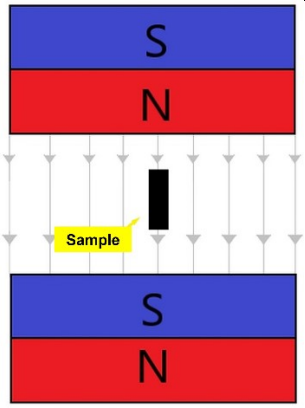

I	Printing with a magnet around the printed area at 45° angle to the field lines	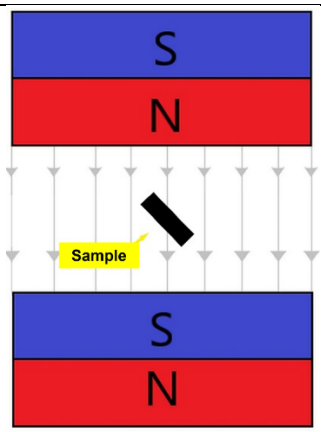
C	Printing on the width of the cube (edge of the magnet) with a 0° angle to the field lines	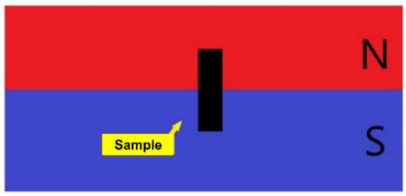
D	Printing on the width of the cube (magnet edge) perpendicular to the field lines	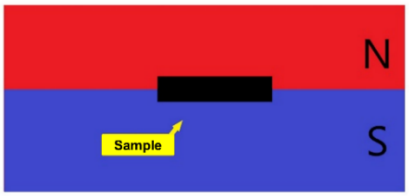
G	Printing on the width of the cube (edge of the magnet) with a 45°angle to the field	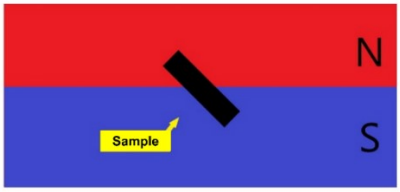
E	Printing on two magnet poles in line with the drawn line	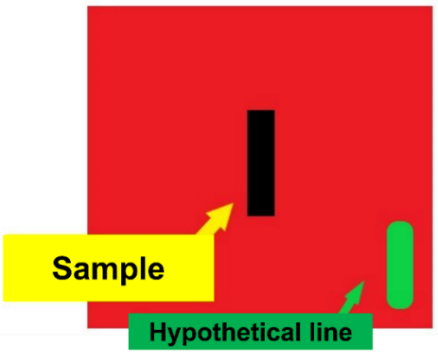
F	Printing on two magnet poles perpendicular to the drawn line	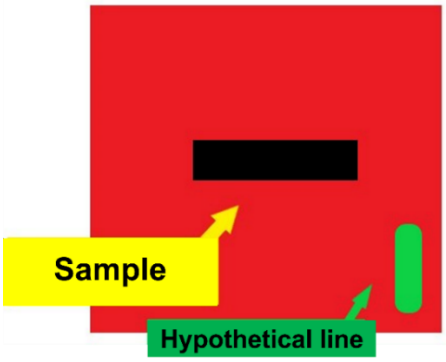

To measure the magnetization of the samples in different states, the VSM made by the Kashan academic magnetism company located in the central chemistry laboratory of Bo Ali-Sina University was used. This machine has a 1.5 Tesla maximum magnetic field capacity. Additionally, this equipment can evaluate samples up to a maximum of five millimetres in length and breadth. The magnetic hysteresis curve of the printed samples was drawn after they underwent magneto-metric examination up to a magnetic field of around 1000 (Oe) at room temperature.

All samples were examined vertically and at 90° angle to the field lines. Origin data analysis software was used to draw graphs of output results. The output results are presented in the form of a loop diagram of specific magnetization hysteresis (emu/g) on the applied field (Oe). It should be noted that in the topics of electromagnetism, the number of magnetic dipoles per unit volume of the object is called magnetization, and the result of dividing the magnetization by the density of the material under study defines the specific magnetization.

2.5. Mechanical testing

In order to investigate the effect of different states of the magnetic field on the mechanical properties of the printed samples, 9 samples were printed in three situations and each in three printing angle patterns in relation to the stretching direction, using a 0.6 mm nozzle diameter, 230 °C nozzle temperature, 45 °C bed temperature, 35 mm/s printing speed, and 0.5 mm outer shell layer thicknesses. The three states of the magnet during sample printing are simple test samples without magnetic field (samples 1-3), test samples with magnets under the printing area (samples 4-6), and test samples with magnets around the printing area (samples 7-9).

It should be noted that in the printing mode between two magnets in state B, the distance between the two magnets was 35.15 mm. Also, in states H and I, due to the need for more space for horizontal movement in the X direction of the printer, the distance between the two magnets was chosen to be approximately 56 mm according to the dimensions of the extruder (see Figure 4(a)). According to the magnets' dimensions, two magnets stuck together from the point where the poles are separated were used in the case of printing with magnets below to produce a magnetic field in the gauge portion of the printed sample as shown in Figure 4(b).

Also, different raster angles are presented in Figure 4(c). Samples are printing lines perpendicular to the stretching direction, printing lines in the direction of tension, and printing lines at angle of 45° to the direction of stretching. In total, the number of samples and their printing conditions are presented in Table 2. To check the mechanical properties of the printed samples, the universal servo electric tensile testing machine (STM-50) with a capacity of 5 tons made by Santam Company was used. The tensile test was followed according to ASTM D630-14 (V) and the sample size is shown in Figure 4(d) [35]. The samples were stretched according to the ASTM D630-14 standard at speed of 1 mm/min and the force diagram was drawn according to the displacement of all the broken samples (see Figure 4(e)). Origin data analysis software was used to draw graphs of output results.

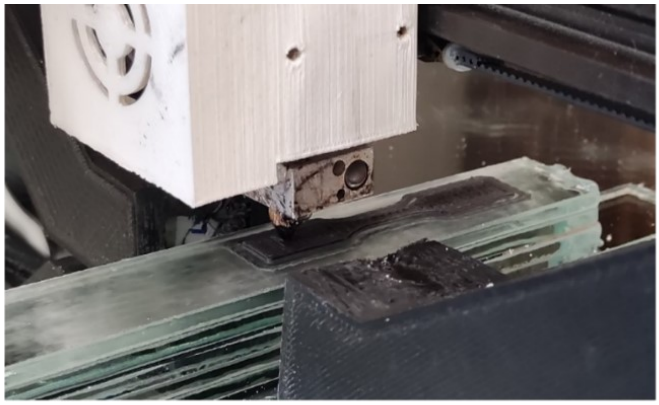

(a)

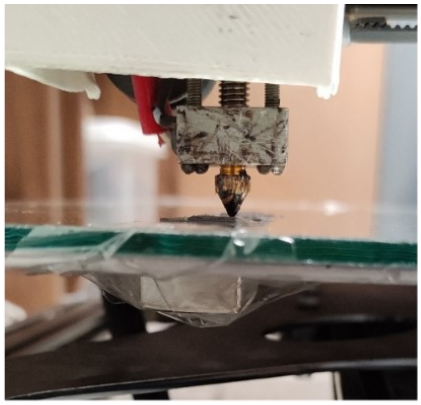

(b)

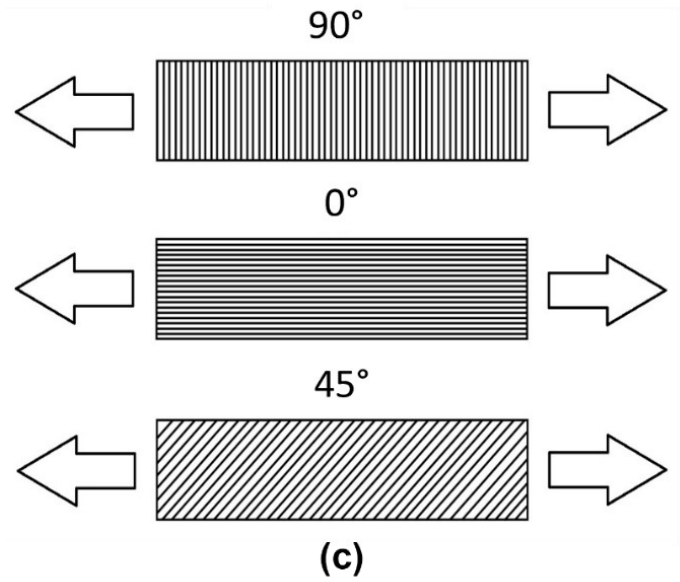

(c)

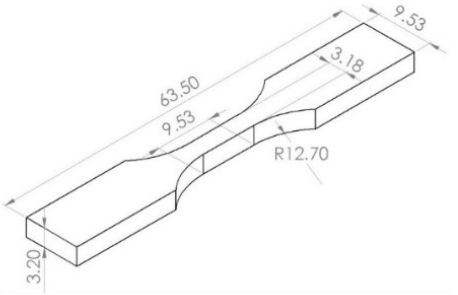

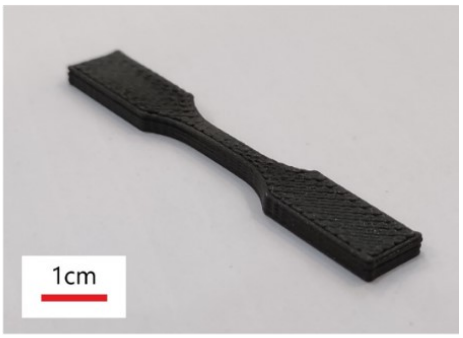

(d)

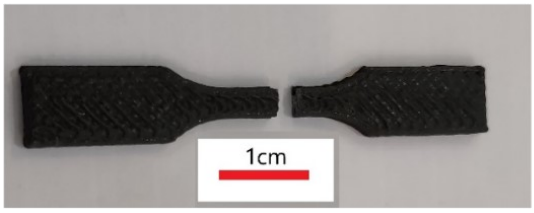

(e)

Figure 4. (a) Print the tensile test sample in print mode between two magnets. **(b)** Print the tensile test sample in print mode with a magnet under the print area. **(c)** Raster angle of tensile test samples. **(d)** Dimensions of the tensile test sample in millimetres based on ASTM D630-14 (V). **(e)** Broken tensile test sample.

Table 2. The number and printing conditions of the printed tensile test samples

Sample	Magnet condition	Printing conditions
1	Without magnet	Lines perpendicular to the direction of tension
2		Lines in line with the direction of tension
3		Lines with 45° to the direction of tension
4	Magnet below	Lines perpendicular to the direction of tension
5		Lines in line with the direction of tension
6		Lines with 45° to the direction of tension
7	Magnets around the print area	Lines perpendicular to the direction of tension
8		Lines in line with the direction of tension
9		Lines with 45° to the direction of tension

2.6. Scanning electron microscope (SEM)

Among the samples, samples number two, five, and eight, which have the highest maximum stress values, were selected for imaging. Due to the variations in the magnetic field states during each sample's printing, the choice of these three samples also allows for the examination of the impact of various magnetic fields. Due to the sections being destroyed during the sample preparation step, imaging of the fracture sections was done first. As was previously stated, samples 2, 5, and 8 were selected at this stage due to the highest breaking force and to compare the condition of iron particles in three states without magnets, magnets below, and magnets around.

Images of fracture sections were prepared at different magnifications. The chosen tensile test samples were prepared for transverse section imaging investigation using a scanning electron microscope (SEM). In this regard, the fracture surface was smoothed by sanding procedure after photographing the sample's fracture sections. The cross-section of the samples was then coated with a thin coating of gold due to the non-conductivity of the fracture cross-section and the lack of iron particles on the surface. An SEM machine was used to capture photographs of the microstructure of the printed samples. This tool can analyse phases, microstructure particles, and elements heavier than aluminium in all metallic and non-metallic materials. To capture photographs of microstructures, this machine also has a professional digital camera.

3. Results and discussions

3.1. VSM results

The VSM test results are examined in this section. The samples' outcomes for each magnet location are first examined independently, and the results are then combined. The output data are shown as a loop diagram of the applied field (Oe) and specific magnetization hysteresis (emu/g). Specific magnetization is the result of dividing the magnetization by the density of the substance being studied in the field of electromagnetism [36].

At first, the results of the samples related to each position of the magnet are checked separately, and then the results are summarized. In general, in the case of placing the magnet around the sample printing area, three samples are made using a personalized printer. At first, sample B was printed with a 90° printing angle to the field lines, between two magnets with a distance of 35.15 mm. Due to the necessity of the transverse movement of the extruder for

the printing process, two samples H and I were printed with 0° and 45° angles to the field lines, respectively. Hence, the distance between the two magnets was 56 mm. The results of all the tests in this mode are presented in Figure 5(a).

As can be seen in Figure 5(a), sample B experiences more saturation magnetization in a lower field than samples H and I, which can be due to the smaller distance between the magnets. As a result, the magnetic field is stronger when this sample was printed. On the other hand, in two samples H and I, the increase of the printing angle compared to the direction of the magnetic field lines during the printing procedure caused the measured saturation-specific magnetization in the sample to be higher. This can be due to the vertical placement of the sample in the VSM test. Because the residual magnetic property of the magnetic field from the magnets in the samples printed at angle of 45° and 90° to the field is in line with the induced field of VSM and increases the specific saturation magnetization in the sample with a printing angle of 45° and 90°. It seems that applying a magnetic field by placing the magnets on both sides of the extruder while printing the sample leads to a lower measured saturation magnetization than the sample printed without a magnetic field.

Five samples are printed when the magnet is placed under the sample printing area. Three samples are printed on the edge of the magnet (the place where the poles are separated) and two samples are printed on the wide surface of the magnet (one of the poles). The samples were printed on the edge of the two magnets with the mentioned parameters. Three samples C, D, and G were printed with 0, 45, and 90° angles relative to the direction of the magnetic field of the magnet, and the corresponding results are presented in Figure 5(b). As can be seen in the results, the graph of sample C with a 0° angle to the field shows higher saturation-specific magnetization compared to other samples. After sample C, sample G is located with a printing angle of 45° to the magnetic field lines. Sample D shows the lowest specific saturation magnetization. In this case, the magnetic field is observed that as the printing angle increases with respect to the direction of the magnetic field lines of the magnet, the saturation magnetization decreases. Comparing the results with the printed sample without a magnetic field, when the magnetic field is applied in the direction of sample deposition (sample C), the specific saturation magnetization of the printed sample in the magnetic field increases by 63.46% compared to the printed sample without a magnetic field, which is in accordance with the results of previous research [26].

In the case of printing on the magnet pole, the samples were printed on the two magnet poles in line with the imaginary line and perpendicular to the imaginary line. According to the results, sample E shows a higher saturation magnetization in a lower field (see Figure 5(c)). While sample F is saturated in a lower field than sample A, it shows lower saturation magnetization than sample A. In general, acceptable coordination between the results is not observed in this case, which can be due to errors in the printing and placement process in the VSM device. For this reason, the printing mode on the separation of the magnet poles was used to print the tensile test samples.

According to the results presented in Figure 5(d), all the tested samples show soft magnetic hysteresis loops, which is consistent with the results of previous studies [26,34]. By comparing the results of all cases with each other in Figure 5(d) and Table 3, the samples printed on the edge of the magnet have the highest specific saturation magnetization compared to other samples. On the other hand, samples printed with magnets around the

printing area are saturated in a lower specific magnetization than samples printed without a magnetic field. It seems that sample E is saturated in less field than other samples, while this sample has a 36.01% increase in specific saturation magnetization compared to the printed sample in the state without a magnetic field. The samples printed on the magnet are saturated in a higher specific magnetization than those printed with magnets.

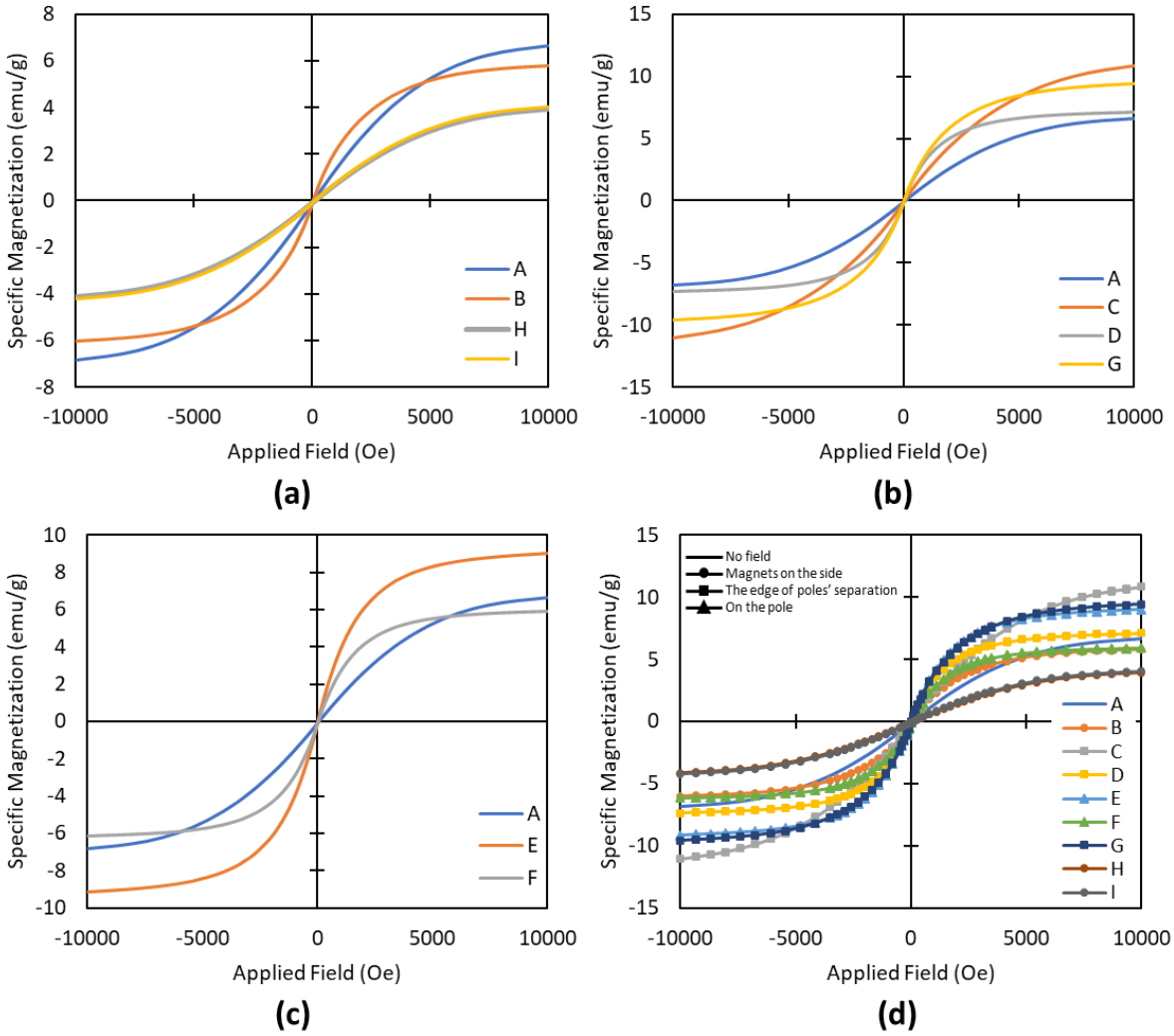

Figure 5. (a) Comparison of the residual loop of samples printed with magnets around and without magnets. A) Printed sample without magnetic field, B) printed sample perpendicular to the field with a magnet around the printing process, H) printed sample with a magnet around the printing process at 0° angle to the field lines, and I) printed sample with magnets around the printing process at 45° angle to the field lines. **(b)** Comparing the residual loop of samples printed on the separation of magnet poles with the sample printed without magnetic field. A) sample printed without magnetic field, C) sample printed on the separation of the magnet poles with 0° angle to the field lines, D) sample printed on the separation of the magnet poles with a perpendicular angle to the field lines, and G) sample Printed on the separation of the magnet poles at angle of 45° to the field lines. **(c)** Comparing the residual loop of samples printed on the magnet pole with the sample printed without a magnetic field. A) Printed sample without magnetic field, E) printed sample on the magnet pole with a 0° angle to the drawn line, and F) printed sample on the magnet pole with a perpendicular angle to the drawn line. **(d)** Comparison of the residual loop of all printed samples with each other.

A) printed sample without magnetic field, B) printed sample perpendicular to the field with a magnet around the printing process, C) printed sample on the separation of the magnet poles with a zero degree angle to the field lines, D) printed sample on The place of separation of the magnet poles with an angle perpendicular to the field lines, E) the sample printed on the magnet pole with a 0° angle to the drawn line, F) the sample printed on the magnet pole with an angle perpendicular to the drawn line, G) the printed sample placed on the separation of the magnet poles at angle of 45° to the field lines, H) the sample printed with a magnet around the printing process at angle of 0 degrees to the field lines, and I) the sample printed with a magnet around the printing process at angle of 45° relative to field lines.

Table 3. Maximum magnetization for printed samples

Sample	Printing mode	Specific saturation magnetization (emu/g)	Applied field (Oe)
A	Printing without any magnetic field	6.63115	10000
B	Printing with a magnet around the printed area perpendicular to the field lines	5.79452	10000
C	Printing on the width of the cube (edge of the magnet) with 0° to the field	10.8392	10000
D	Printing on the width of the cube (magnet edge) perpendicular to the field	7.12043	10000
E	Printing on two magnet poles in line with the drawn line	9.02498	10000
F	Printing on two magnet poles perpendicular to the drawn line	5.91823	10000
G	Printing on the width of the cube (edge of the magnet) with an angle of 45 degrees to the field	9.43006	10000
H	Printing with a magnet around 0° to the field	3.94614	10000
I	Printing with the magnet around at angle of 45° to the field	4.04158	10000

3.2. Analysis of tensile test results

In this section, the samples printed in each mode are compared with each other to check the effect of the printing angle in relation to the stretching direction. The printed samples with the same angles and different magnetic field states are compared to study the effect of the magnetic field on the mechanical properties of the printed samples.

According to the tensile test results of the printed samples without magnetic field which is shown in Figure 6(a). Sample 2 with a printing angle of 0° compared to the stretching direction has more tensile strength than samples 1 and 3 with printing angles of 90° and 45° compared to the stretching direction. This is because the printed filament is stronger than the connection of printed lines in samples with printing angles of 45° and 90° to the stretching direction. In fact, it can be concluded that the adhesion strength between printed lines is relatively lower than the strength of the printed line itself, which is in accordance with previous studies, apart from the type of filament used in this study [37–39].

The results presented in Figure 6(b) confirm all the discussions raised in the printing mode without the magnetic field. In contrast to the case without the magnetic field, it can be seen in Figure 6(b) that the elongation in the stretch area of sample 4 with print lines at 90° to the stretch direction is 36.68% less than the sample with 0° angle. According to Figure 6(c), the sample printed with a 0° angle to the stretching direction has more tensile strength than the others like previous sets.

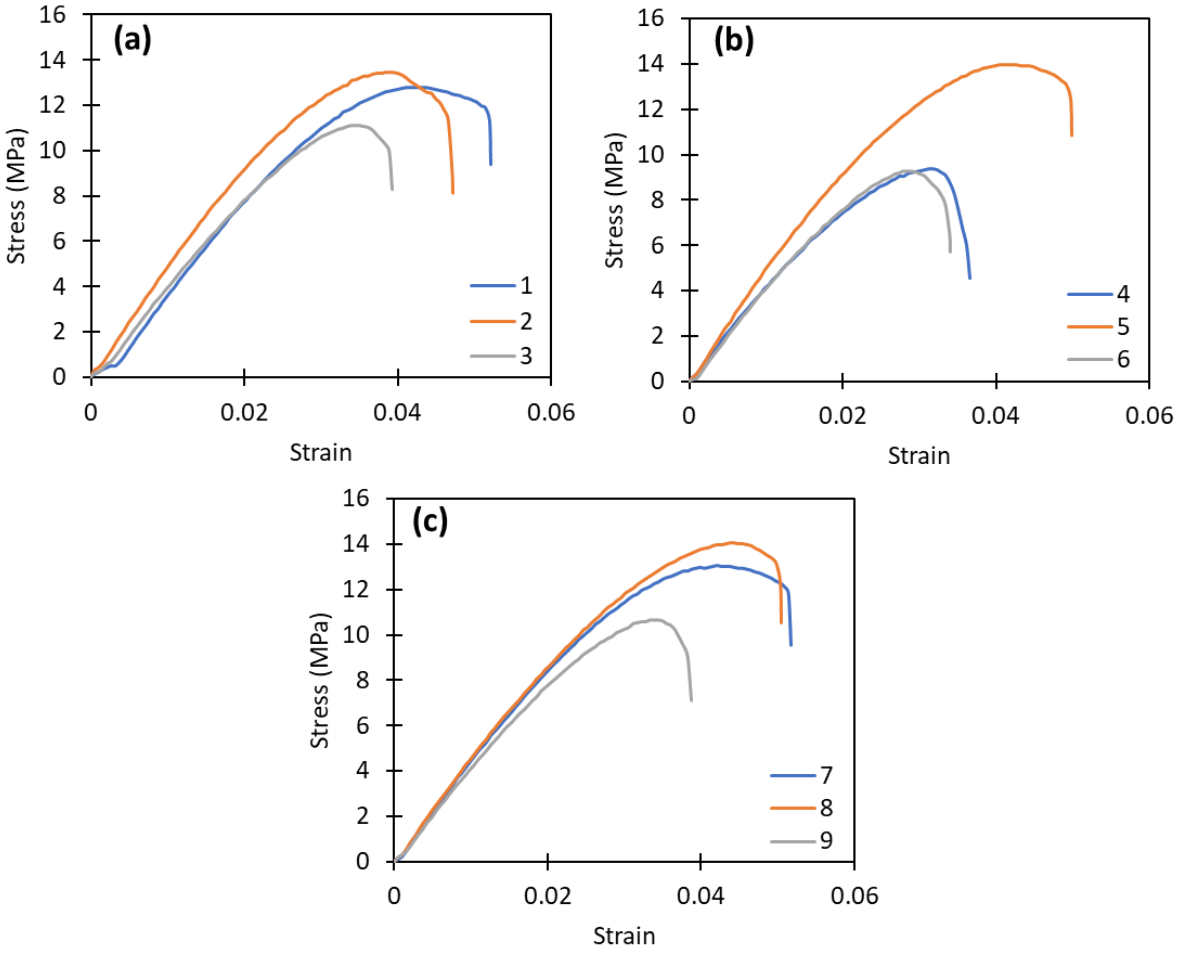

Figure 6. (a) Tensile test results of printed samples without magnetic field. 1) Sample printed with printing lines perpendicular to the stretching direction, 2) sample printed with printing lines aligned with the stretching direction, and 3) sample printed with printing lines at angle of 45° to the stretching direction **(b)** The results of the tensile test of samples printed with a magnet under the printing area. 4) Sample printed with a magnet under the printing area with printing lines perpendicular to the direction of tension, 5) sample printed with a magnet under the printing area with printing lines in line with the direction of stretching, and 6) sample printed with a magnet under the printing area with printing lines with an angle of 45° to the direction of stretching **(c)** Tensile test results of samples printed with magnets around the printing area. 7) Sample printed with a magnet around the printing area with printing lines perpendicular to the direction of tension, 8) Sample printed with a magnet around the printing area with printing lines in line with the direction of stretching, and 9) sample printed with a magnet around the printing area with printing lines with an angle of 45° to the direction of stretching.

In order to study the effect of the magnetic field on the mechanical properties of the sample in the same printing parameters, the samples with the same printing angle and variable magnetic field conditions are compared. The SEM photos taken from the fracture surface of the samples are used to investigate the effect of the magnetic field more precisely. The stress-strain diagrams of the printed samples at angle of 90° to the direction of tension are shown in Figure 7(a). At this angle, the presence of the magnetic field caused by the magnet around the printing area has increased the strength of the printed sample by 1.9% compared to the printing state without a magnetic field. While the presence of a magnet under the printed sample reduces the strength of the printed sample by 26.89%. Therefore, it can be concluded that in the printing angle of 90°, the use of magnets around the sample printing process increases the adhesion strength of the printing lines compared to the case without magnetic fields. Also, in the same way for printing with a magnet under the sample printing process, it can be concluded that the presence of a magnet under the printing area reduces the adhesive strength of the printed lines.

According to Table 4, the printing angle of 0° compared to the stretching direction in all cases results in the highest strength in the output sample. For comparison, graphs of samples printed with a 0°angle are presented in Figure 7(b). In general, the magnetic field increases the mechanical properties of the printed samples at this angle. At this angle, in the case of a magnet around the printing area (sample 8), due to the magnetization of the line being printed and the printed line (see Figure 7(c)), the attraction force is created between the opposite poles of the lines, and this can cause more adhesion of the lines, decrease the porosity in the printed sample and increase the strength of the sample by 21.4% compared to the printing mode without magnetic field.

As can be seen in Figure 7(d), at angle of 45°, the printed sample without a magnetic field shows the highest stress. The next highest stress is the sample printed with magnets around the print area. In this angle, like the 90° angle, the sample printed with a magnet shows the lowest strength under the printed area of the sample. In fact, it can be concluded that at printing angle of 45° compared to the direction of tension, the presence of a magnet around and under the printing area of the sample reduces the strength of the printed sample by 4 and 16.72%, respectively, compared to the printing mode without magnetic field.

According to Table 4, the presence of a magnet under the printed area of the sample increases by 62.3% the maximum stress of the sample with a printing angle of 0°, compared to the printing without magnets. Also, the use of a magnet under the printed area of the sample at this angle leads to an increase in strength. At the printing angles of 45 and 90°, in contrast to the 0° angle, the reduction of the maximum stress is observed, and the sample printed with a magnet under the printing area shows a lower tensile strength than the case without a magnet. In the case of printing with a magnet under the sample, the difference in the value of the maximum stress between the sample with a 0° angle and the samples with 90° and 45° angles is greater than in the case of printing without a magnet. In fact, the presence of a magnetic field during the printing process reduces the adhesion strength between the printed lines.

In this instance, since all conditions are the same aside from the magnetic field condition, this difference can be attributed due to the presence of the magnetic field under the sample, the movement of iron particles, and the orientation of the magnetic dipoles in the molten

filament during the printing process under the influence of the magnetic field. Printing with a magnet around the printing area, the difference in the values of the maximum stress between the 0° angle and the 90° and 45° angles is less than the case of the magnet under the sample, and in this aspect, it is like the case without a magnetic field.

According to Table 4, the samples made at 0° and 90° angles have higher tensile strength than those in the printing mode without a magnetic field. In fact, the presence of the magnetic field around the print area, printing angles of 0° and 90°, increases the tensile strength of the printed sample. The samples printed with magnets around the printing area show a higher maximum stress compared to the samples printed with magnets under the printing area. Apart from the influence of the printing angle, the use of two magnets around the printing area provides better mechanical properties in the manufactured sample than the magnet under the printing area.

SEM images of fracture sections of 2, 5, and 8 samples are presented in Figure 8(a). As can be seen, in sample 2, there is a longitudinal discontinuity of the printed lines and porosity, which can be the reason for the lower strength of the printed sample compared to the other two samples. No longitudinal discontinuity can be seen in samples 5 and 8. According to Figure 8(b), the width of the printed layers of sample 5 decreases with increasing height, which can be due to the presence of a magnet under the sample. The edges of the eight sample layers have more alignment in the vertical direction. By examining the SEM images of the prepared samples in Figures 8(a) and (b), it is possible to see the movement of iron particles in the magnetic field, especially in printing with a magnet under the printed area of the sample. Slight sedimentation of iron particles can be seen in some parts of these samples.

The obtained results are useful in terms of activation with lower magnetic field strength. The printed structure can be activated with less field strength if magnets are placed below the printing bed. Hence, the power consumption would be less in terms of shape morphing and activating the structure [40]. Also, the results show the mechanical properties of printed specimens increased by applying a magnetic field during the printing procedure. Thus, printed structures can be stronger while less magnetic field strength is required to stimulate them [41]. The results are useful in terms of shape programming with less input field power and the metamaterial scaffolds are stronger in different applications [22,23].

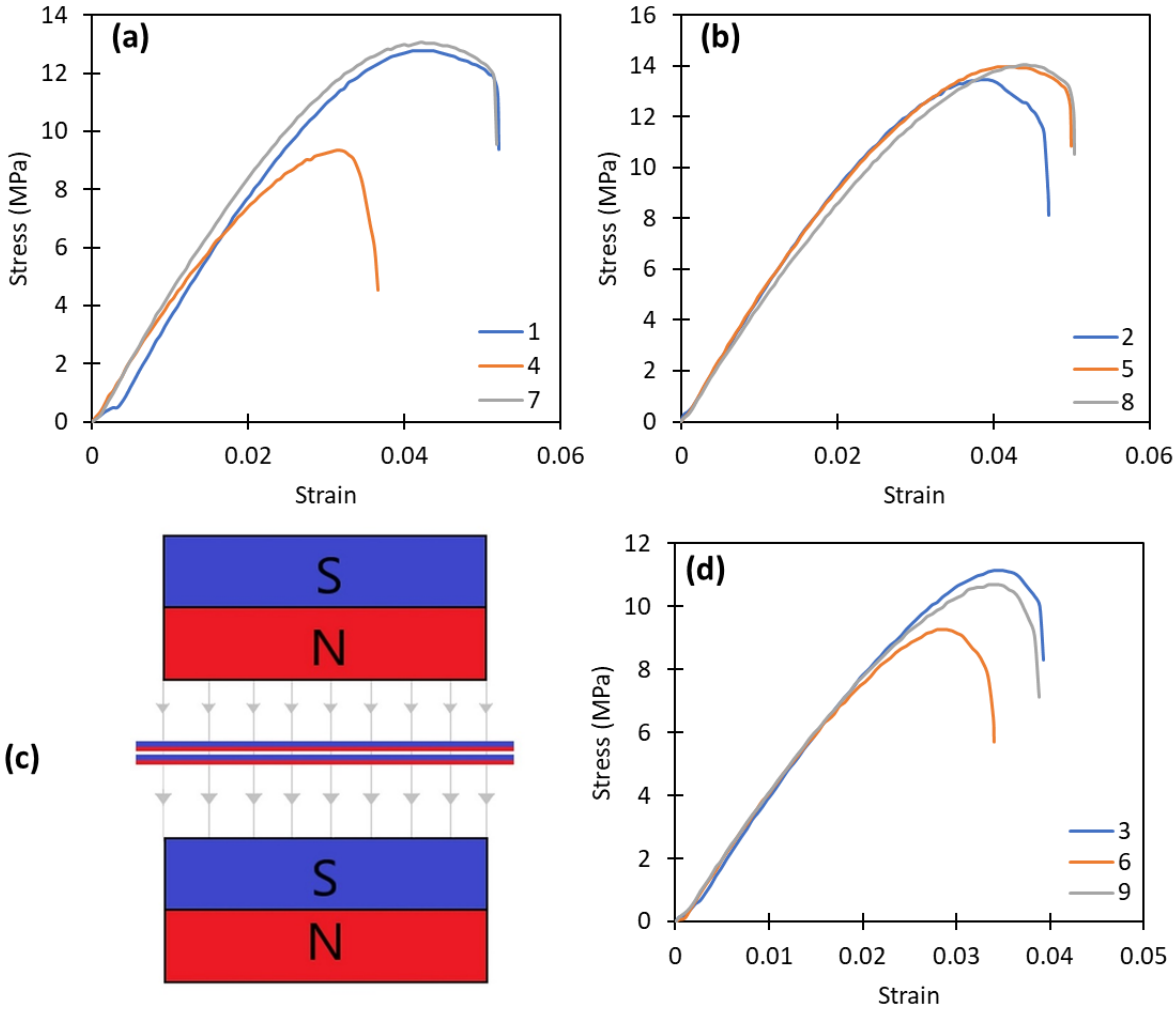

Figure 7. (a) The tensile test results of the samples printed at angle of 90° to the tensile direction, 1) printed sample without magnetic field at angle of 90° to the direction of stretching, 4) sample printed with a magnet under the printing area with an angle of 90° to the direction of stretching, and 7) sample printed with a magnet around the printing area with an angle of 90° to the direction of tension. **(b)** Tensile test results of printed samples with a 0° angle of print lines relative to the tensile direction, 2) the printed sample without magnetic field with the angle of the print lines of 0° relative to the direction of tension, 5) the sample printed with a magnet under the printing area with the angle of the print lines of 0° relative to the direction of tension, and 8) the sample printed with the magnet in around the printing area with the angle of the printing lines of 0° to the direction of tension. **(c)** The force of attraction between the magnetized lines in the magnet state around the printing area (grey lines show the direction of the magnetic field). **(d)** Tensile test results of samples printed at angle of 45° to the direction of tension, 3) printed sample without a magnetic field with an angle of the printing lines of 45° to the direction of tension, 6) Sample printed with a magnet under the printing area with an angle of the printing lines of 45° to the direction of tension, 9) Sample printed with a magnet in around the printing area with the angle of the printing lines at 45° to the direction of tension

Table 4. The maximum value of the stress-strain diagram of the printed samples

Sample	Magnet condition	Printing conditions	Stress (MPa)	Strain
1	Without magnet	Lines perpendicular to the direction of tension	12.79	0.0438
2		Lines in line with the direction of tension	13.47	0.0471
3		Lines with 45° to the direction of tension	11.13	0.0393
4	Magnet below	Lines perpendicular to the direction of tension	9.35	0.0367
5		Lines in line with the direction of tension	13.96	0.052
6		Lines with 45° to the direction of tension	9.27	0.0341
7	Magnets around the print area	Lines perpendicular to the direction of tension	13.07	0.0518
8		Lines in line with the direction of tension	14.04	0.0504
9		Lines with 45° to the direction of tension	10.68	0.0388

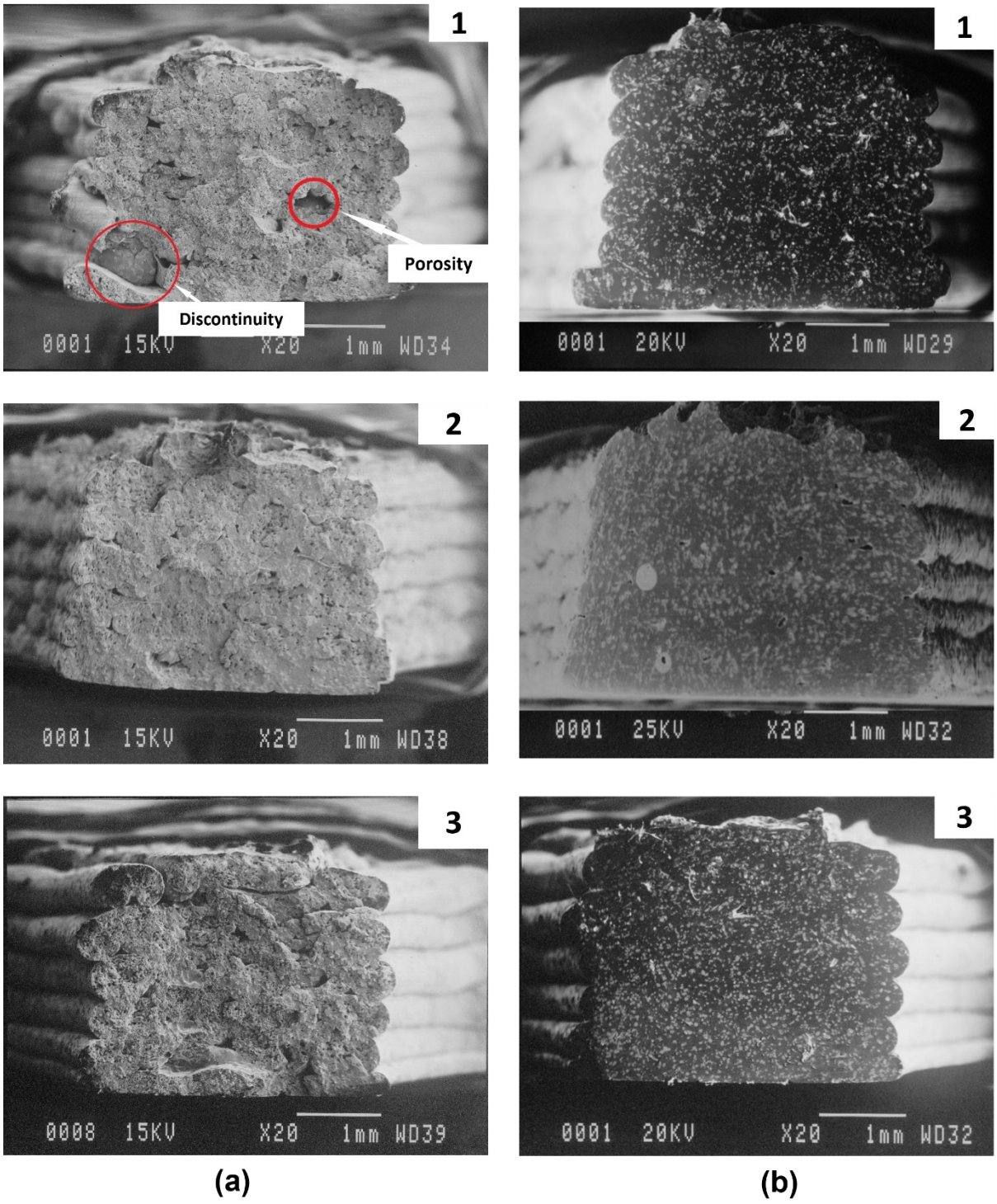

Figure 8. (a) Fracture sections of printed samples with 0° angle. 1) sample 2, printed without magnetic field, 2) sample 5, printed with a magnet under the sample area and 3) sample 8, printed with a magnet around the print area. **(b)** Prepared fracture sections of printed samples with 0° angle. 1) sample 2, printed without magnetic field, 2) sample 5, printed with a magnet under the sample location and 3) sample 8, printed with a magnet around the print location

4. Conclusions

In this research, the influence of the magnetic field state and the angle of the 3D printing with respect to the magnetic field lines and the angle of the printing lines with respect to the stretching direction on the magnetic and mechanical properties of the printed samples have been investigated. The application of this work is in the 4D printing field in which the stimulation and activation of structures with high strength are necessary. The general results obtained from the tests are as follows:

- In the case of printing with a magnet around the printed area of the sample, increasing the printing angle compared to the direction of the magnetic field lines during printing causes the measured saturation magnetization to be higher in the sample.
- Applying a magnetic field by magnets on both sides of the extruder while printing the sample lead to a lower measured saturation magnetization with the value of 3.94614 emu/g compared to the sample printed without a magnetic field with the value of 6.63115 emu/g.
- In the case of printing on the width (edge) of the magnet, as the angle of the magnetic field increases with respect to the direction of the magnetic field lines, the saturation magnetization decreases to 7.12043 emu/g.
- Comparing the results with the printed sample without a magnetic field, when the magnetic field is applied in the direction of the sample deposition, the specific saturation magnetization of the printed sample increases by 63.46% in the magnetic field.
- In general, the samples printed on the magnet are saturated in a higher specific magnetization than the samples printed with magnets around them.
- The sample printed with a 0° angle to the stretching direction has more tensile strength than other samples with values between 13 to 14.04 MPa. In fact, the adhesion strength between printed lines is relatively lower than the strength of the printed line itself.
- When the magnet is placed around the printing area, at 0° angle to the direction of tension, due to the magnetization of the line being printed and the printed line, the force of attraction is created between the opposite poles of the lines, and this causes more adhesion of lines, reduction of porosity in the printed sample and increase of 21.4% strength of the sample compared to the printing mode without magnetic field.
- In the printing angle of 0°, using a magnet around the sample printing process increases the adhesion strength with the value of 14.04 MPa of the printing lines compared to the case without a magnetic field.
- The presence of a magnet weakens the adhesion strength of the printed lines in the sample printing process when printing with a magnet.
- The presence of a magnetic field under the printing area when printing a sample with a 0° angle to the stretching direction increases the strength of the printed line to 13.96 MPa.

- According to the SEM image of the fracture area of the sample printed with a 0° angle compared to the magnet pull direction under the printing area (sample five), the width of the printed layers with a 0° printing angle decreases with an increase in height, which can be due to the presence of a magnet under the sample.
- In general, the samples printed with magnets around the print site show a higher maximum failure compared to the samples printed with magnets below the print site. It can be concluded that apart from the influence of the printing angle, the use of two magnets around the printing area provides better mechanical properties in the manufactured sample than the magnet under the printing area.
- It is possible to choose the printing mode with a 0° angle to the direction of stretching with the magnet under the printing area of the sample as the best mode to achieve the desired magnetic and mechanical properties.

Declaration of Competing Interest

The authors declare that they have no known competing financial interests or personal relationships that could have appeared to influence the work reported in this paper.

References

[1] S. Singh, S. Ramakrishna, R. Singh, Material issues in additive manufacturing: A review, J Manuf Process. 25 (2017). https://doi.org/10.1016/j.jmapro.2016.11.006.

[2] M. Lalegani Dezaki, M.K.A. Mohd Ariffin, S. Hatami, An overview of fused deposition modelling (FDM): research, development and process optimisation, Rapid Prototyp J. 27 (2021) 562–582. https://doi.org/10.1108/RPJ-08-2019-0230.

[3] D. Srinivasan, M. Meignanamoorthy, M. Ravichandran, V. Mohanavel, S. v. Alagarsamy, C. Chanakyan, S. Sakthivelu, A. Karthick, T.R. Prabhu, S. Rajkumar, 3D Printing Manufacturing Techniques, Materials, and Applications: An Overview, Advances in Materials Science and Engineering. 2021 (2021). https://doi.org/10.1155/2021/5756563.

[4] I. Gibson, D. Rosen, B. Stucker, M. Khorasani, Material Extrusion, in: I. Gibson, D. Rosen, B. Stucker, M. Khorasani (Eds.), Additive Manufacturing Technologies, Springer International Publishing, Cham, 2021: pp. 171–201. https://doi.org/10.1007/978-3-030-56127-7_6.

[5] E.H. Tümer, H.Y. Erbil, Extrusion-based 3d printing applications of pla composites: A review, Coatings. 11 (2021). https://doi.org/10.3390/coatings11040390.

[6] Z. Liu, Y. Wang, B. Wu, C. Cui, Y. Guo, C. Yan, A critical review of fused deposition modeling 3D printing technology in manufacturing polylactic acid parts, International Journal of Advanced Manufacturing Technology. 102 (2019). https://doi.org/10.1007/s00170-019-03332-x.

[7] V. Cojocaru, D. Frunzaverde, C.-O. Miclosina, G. Marginean, The influence of the process parameters on the mechanical properties of PLA specimens produced by fused

filament fabrication—A review, Polymers (Basel). 14 (2022) 886. https://doi.org/10.3390/polym14050886.

[8] M. Bodaghi, A.R. Damanpack, W.H. Liao, Adaptive metamaterials by functionally graded 4D printing, Mater Des. 135 (2017). https://doi.org/10.1016/j.matdes.2017.08.069.

[9] S.J.M. van Vilsteren, H. Yarmand, S. Ghodrat, Review of Magnetic Shape Memory Polymers and Magnetic Soft Materials, Magnetochemistry. 7 (2021) 123. https://doi.org/10.3390/magnetochemistry7090123.

[10] Q. Ze, X. Kuang, S. Wu, J. Wong, S.M. Montgomery, R. Zhang, J.M. Kovitz, F. Yang, H.J. Qi, R. Zhao, Magnetic Shape Memory Polymers with Integrated Multifunctional Shape Manipulation, Advanced Materials. 32 (2020). https://doi.org/10.1002/adma.201906657.

[11] S.Y. Hann, H. Cui, M. Nowicki, L.G. Zhang, 4D printing soft robotics for biomedical applications, Addit Manuf. 36 (2020) 101567. https://doi.org/10.1016/j.addma.2020.101567.

[12] M. Aberoumand, D. Rahmatabadi, A. Aminzadeh, M. Moradi, 4D Printing by Fused Deposition Modeling (FDM), in: H.K. Dave, J.P. Davim (Eds.), Fused Deposition Modeling Based 3D Printing, Springer International Publishing, Cham, 2021: pp. 377–402. https://doi.org/10.1007/978-3-030-68024-4_20.

[13] M.Y. Khalid, Z.U. Arif, W. Ahmed, R. Umer, A. Zolfagharian, M. Bodaghi, 4D printing: Technological developments in robotics applications, Sens Actuators A Phys. 343 (2022) 113670. https://doi.org/https://doi.org/10.1016/j.sna.2022.113670.

[14] M.Y. Khalid, Z.U. Arif, R. Noroozi, A. Zolfagharian, M. Bodaghi, 4D printing of shape memory polymer composites: A review on fabrication techniques, applications, and future perspectives, J Manuf Process. 81 (2022) 759–797. https://doi.org/https://doi.org/10.1016/j.jmapro.2022.07.035.

[15] J.C. Breger, C. Yoon, R. Xiao, H.R. Kwag, M.O. Wang, J.P. Fisher, T.D. Nguyen, D.H. Gracias, Self-folding thermo-magnetically responsive soft microgrippers, ACS Appl Mater Interfaces. 7 (2015). https://doi.org/10.1021/am508621s.

[16] Z. Zhang, K.G. Demir, G.X. Gu, Developments in 4D-printing: a review on current smart materials, technologies, and applications, Int J Smart Nano Mater. 10 (2019). https://doi.org/10.1080/19475411.2019.1591541.

[17] M.L. Dezaki, M. Bodaghi, Soft Magneto-Responsive Shape Memory Foam Composite Actuators, Macromol Mater Eng. (2022) 2200490. https://doi.org/10.1002/mame.202200490.

[18] M. Ralchev, V. Mateev, I. Marinova, Magnetic properties of FFF/FDM 3D printed magnetic material, in: 2021 17th Conference on Electrical Machines, Drives and Power Systems, ELMA 2021 - Proceedings, 2021. https://doi.org/10.1109/ELMA52514.2021.9503037.

[19] Y. Zhang, Q. Wang, S. Yi, Z. Lin, C. Wang, Z. Chen, L. Jiang, 4D Printing of Magnetoactive Soft Materials for On-Demand Magnetic Actuation Transformation, ACS Appl Mater Interfaces. 13 (2021). https://doi.org/10.1021/acsami.0c19280.

[20] E. Yarali, M. Baniasadi, A. Zolfagharian, M. Chavoshi, F. Arefi, M. Hossain, A. Bastola, M. Ansari, A. Foyouzat, A. Dabbagh, M. Ebrahimi, M.J. Mirzaali, M. Bodaghi, Magneto-/electro-responsive polymers toward manufacturing, characterization, and biomedical/soft robotic applications, Appl Mater Today. 26 (2022) 101306. https://doi.org/10.1016/j.apmt.2021.101306.

[21] K.S. Riley, K.J. Ang, K.A. Martin, W.K. Chan, J.A. Faber, A.F. Arrieta, Encoding multiple permanent shapes in 3D printed structures, Mater Des. 194 (2020). https://doi.org/10.1016/j.matdes.2020.108888.

[22] F. Zhang, L. Wang, Z. Zheng, Y. Liu, J. Leng, Magnetic programming of 4D printed shape memory composite structures, Compos Part A Appl Sci Manuf. 125 (2019) 105571. https://doi.org/10.1016/j.compositesa.2019.105571.

[23] H. Liu, F. Wang, W. Wu, X. Dong, L. Sang, 4D printing of mechanically robust PLA/TPU/Fe3O4 magneto-responsive shape memory polymers for smart structures, Compos B Eng. 248 (2023) 110382. https://doi.org/10.1016/j.compositesb.2022.110382.

[24] M. Lalegani Dezaki, M. Bodaghi, Magnetorheological elastomer-based 4D printed electroactive composite actuators, Sens Actuators A Phys. 349 (2023) 114063. https://doi.org/10.1016/j.sna.2022.114063.

[25] A. Kafle, E. Luis, R. Silwal, H.M. Pan, P.L. Shrestha, A.K. Bastola, 3D/4D Printing of Polymers: Fused Deposition Modelling (FDM), Selective Laser Sintering (SLS), and Stereolithography (SLA), Polymers (Basel). 13 (2021) 3101. https://doi.org/10.3390/polym13183101.

[26] L. Henderson, S. Zamora, T.N. Ahmed, C. Belduque, J. Tate, M. Yihong Chen, W.J. Geerts, Altering magnetic properties of iron filament PLA using magnetic field assisted additive manufacturing (MFAAM), J Magn Magn Mater. 538 (2021) 168320. https://doi.org/10.1016/j.jmmm.2021.168320.

[27] W. Zhao, F. Zhang, J. Leng, Y. Liu, Personalized 4D printing of bioinspired tracheal scaffold concept based on magnetic stimulated shape memory composites, Compos Sci Technol. 184 (2019). https://doi.org/10.1016/j.compscitech.2019.107866.

[28] C. Ma, S. Wu, Q. Ze, X. Kuang, R. Zhang, H.J. Qi, R. Zhao, Magnetic Multimaterial Printing for Multimodal Shape Transformation with Tunable Properties and Shiftable Mechanical Behaviors, ACS Appl Mater Interfaces. 13 (2021). https://doi.org/10.1021/acsami.0c13863.

[29] M. Moradi, A. Aminzadeh, D. Rahmatabadi, A. Hakimi, Experimental investigation on mechanical characterization of 3D printed PLA produced by fused deposition modeling (FDM), Mater Res Express. 8 (2021). https://doi.org/10.1088/2053-1591/abe8f3.

[30] M. Moradi, A. Aminzadeh, D. Rahmatabadi, S.A. Rasouli, Statistical and Experimental Analysis of Process Parameters of 3D Nylon Printed Parts by Fused Deposition

Modeling: Response Surface Modeling and Optimization, J Mater Eng Perform. 30 (2021). https://doi.org/10.1007/s11665-021-05848-4.

[31] X. Ye, C. Yang, E. He, P. Yang, Q. Gao, T. Yan, S. Yin, Y. Ye, H. Wu, Electromagnetic wave absorption properties of the FeSiAl/PLA and FeSiAl-MoS2-Graphene/PLA double-layer absorber formed by fused deposition modeling, J Magn Magn Mater. (2022) 170280. https://doi.org/10.1016/j.jmmm.2022.170280.

[32] L.M. Bollig, P.J. Hilpisch, G.S. Mowry, B.B. Nelson-Cheeseman, 3D printed magnetic polymer composite transformers, J Magn Magn Mater. 442 (2017). https://doi.org/10.1016/j.jmmm.2017.06.070.

[33] N.A. Fischer, A.L. Robinson, T.J. Lee, T.M. Calascione, L. Koerner, B.B. Nelson-Cheeseman, Magnetic annealing of extruded thermoplastic magnetic elastomers for 3D-Printing via FDM, J Magn Magn Mater. 553 (2022). https://doi.org/10.1016/j.jmmm.2022.169266.

[34] L.M. Bollig, M. v. Patton, G.S. Mowry, B.B. Nelson-Cheeseman, Effects of 3-D Printed Structural Characteristics on Magnetic Properties, IEEE Trans Magn. 53 (2017). https://doi.org/10.1109/TMAG.2017.2698034.

[35] ASTM-D638-14, Standard Test Method for Tensile Properties of Plastics, ASTM Standards. (2014).

[36] T.M. El-Alaily, M.K. El-Nimr, S.A. Saafan, M.M. Kamel, T.M. Meaz, S.T. Assar, Construction and calibration of a low cost and fully automated vibrating sample magnetometer, J Magn Magn Mater. 386 (2015) 25–30. https://doi.org/10.1016/j.jmmm.2015.03.051.

[37] S. Kasmi, G. Ginoux, S. Allaoui, S. Alix, Investigation of 3D printing strategy on the mechanical performance of coextruded continuous carbon fiber reinforced PETG, J Appl Polym Sci. 138 (2021). https://doi.org/10.1002/app.50955.

[38] T. Liu, L. Liu, C. Zeng, Y. Liu, J. Leng, 4D printed anisotropic structures with tailored mechanical behaviors and shape memory effects, Compos Sci Technol. 186 (2020). https://doi.org/10.1016/j.compscitech.2019.107935.

[39] M.S. Meiabadi, M. Moradi, M. Karamimoghadam, S. Ardabili, M. Bodaghi, M. Shokri, A.H. Mosavi, Modeling the producibility of 3d printing in polylactic acid using artificial neural networks and fused filament fabrication, Polymers (Basel). 13 (2021). https://doi.org/10.3390/polym13193219.

[40] S. Joshi, K. Rawat, K. C, V. Rajamohan, A.T. Mathew, K. Koziol, V. Kumar Thakur, B. A.S.S, 4D printing of materials for the future: Opportunities and challenges, Appl Mater Today. 18 (2020) 100490. https://doi.org/10.1016/j.apmt.2019.100490.

[41] P. Zhu, W. Yang, R. Wang, S. Gao, B. Li, Q. Li, 4D Printing of Complex Structures with a Fast Response Time to Magnetic Stimulus, ACS Appl Mater Interfaces. 10 (2018). https://doi.org/10.1021/acsami.8b12853.